WCTE 2016
World Conference on Timber Engineering
August 22-25, 2016 | Vienna, Austria

REINFORCEMENT OF ROUND HOLES IN GLULAM BEAMS ARRANGED ECCENTRICALLY OR IN GROUPS

Martin Danzer[1], Philipp Dietsch[2], Stefan Winter[3]

ABSTRACT: Experimental and numerical investigations on round holes in glulam beams are presented. These were conducted in order to extend the field of practical application, to study the structural behaviour of holes arranged eccentrically or in groups and to generate basic results for deriving a design format. Within these investigations the influence of parameters like eccentricity, clear distance between holes or effect of reinforcement by fully threaded self-tapping screws was considered. A comparison of estimated load-bearing capacities on the basis of the Weibull theory and test results shows good agreement. Strain gauge measurements in reinforcing elements confirm the validity of the chosen methods.

KEYWORDS: Glued laminated timber, holes, holes arranged eccentrically, groups of holes, reinforcement, self-tapping screw

1 INTRODUCTION

In roof structures made of glulam beams, pipes for ventilation or heating are commonly located in the construction level due to architectural reasons or use-related requirements. Therefore the penetration of the glulam beams often cannot be avoided. With regard to designing corresponding holes in glulam beams, the European timber design code Eurocode 5 does not contain a design format. The German National Annex to Eurocode 5, DIN EN 1995-1-1/NA:2013-08, provides design and construction rules for holes in beams as non-contradictory information (NCI). These, however, restrict the positioning of the holes considerably, see Figure 1. In order to extend the field of practical application, a research project with numerical and experimental investigations on round holes in glulam beams arranged eccentrically or in groups is currently in process. Within these investigations, the unreinforced as well as the reinforced state by fully threaded self-tapping screws is considered.

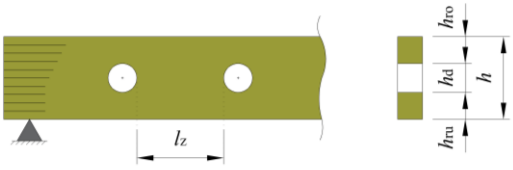

	without reinforcement	with reinforcement
l_z	$\geq$ max (1.5h; 300 mm)	$\geq$ max (1.0h; 300 mm)
$h_{ro(ru)}$	$\geq 0.35h$	$\geq 0.25h$

Figure 1: *Geometrical limitations regarding eccentricity and clear distance according to DIN EN 1995-1-1/NA:2013-08*

2 EXPERIMENTAL INVESTIGATIONS

2.1 MATERIALS AND METHODS

The test configuration for experimental investigations of the above-mentioned parameters is given in Figure 2. The number of specimens per configuration was three.
Regarding the location of the holes in longitudinal direction it was decided to concentrate on the region near the supports, dominated by shear forces, simultaneously complying with sufficient distance to the supports to exclude the influence of load transfer ($M/V = 1.5h$). The eccentricity over the beam height was varied in four steps ($e/h = \pm 0.175, \pm 0.100$), each of them violating the current limits shown in Figure 1. To enable a comparison between single holes and groups of holes arranged in horizontal direction, a consistent hole diameter $d/h = 0.35$ was chosen for these configurations.
For the group of holes arranged horizontally, the clear distance between the holes was reduced in three steps ($l_z = 1.05h,\ 0.70h,\ 0.35h$), also violating the current limits shown in Figure 1. The hole at the location $M/V = 1.5h$ was kept fix, whereas the location of the holes located further away from the support was varied.
Concerning groups of holes arranged in vertical direction, only one configuration featuring a smaller diameter $d/h = 0.25$ was tested due to the fewer possibilities in variation given by the geometry.

[1] Martin Danzer, Email: danzer@tum.de
[2] Philipp Dietsch, Email: dietsch@tum.de
[3] Stefan Winter, Email: winter@tum.de

TU München, Chair for Timber Structures and Building Construction, Arcisstr. 21, D-80333 München

With the intention of a comparison between the group of holes arranged in vertical direction and single holes, the test program was extended to additional tests with holes of a diameter $d/h = 0.25$ and different eccentricities ($e/h = \pm 0.225$, ± 0.100). Referring to the approach reported in [1], 10 out of 12 specimens were tested two times by recycling already tested specimens according to the procedure displayed in Figure 2. For the remaining two specimens new material was used.

Regarding reinforcement fully threaded self-tapping screws according to [2] with a nominal diameter $d = 10$ mm were used. The inclination between screw axis and fibre direction was set to $\alpha = 60°$ in most cases, except $\alpha = 90°$ in case of the vertical group. The objective was to generate a reinforcing effect with regard to both stresses, tension perpendicular to the grain and shear, i.e. the reinforcement was arranged to be as close to the corresponding stress trajectories as possible.

The material used was glulam GL 28h, obtained by two manufacturers. For all configurations, the cross-sectional dimensions were $b \times h = 120 \times 400$ mm. After delivery, the beams were stored in the normal climate of the air-conditioned testing hall. At the time of the experiments, the average moisture content of the specimens was $MC_m = 11.8\%$ ($CoV = 10.7\%$), the average density $\rho_m = 465\,kg/m^3$ ($CoV = 3.0\%$).

The test set-up corresponded to a 3-point bending test, which was carried out displacement-controlled at a constant rate. The loading procedure was according to DIN EN 26891:1991-07, testing the beams with selected load levels of $F = 60$ kN and $F = 15$ kN (load application to $0.4F_{est}$, held constant for 30 s, load reduction to $0.1F_{est}$, held constant for 30 s, load increase until fracture).

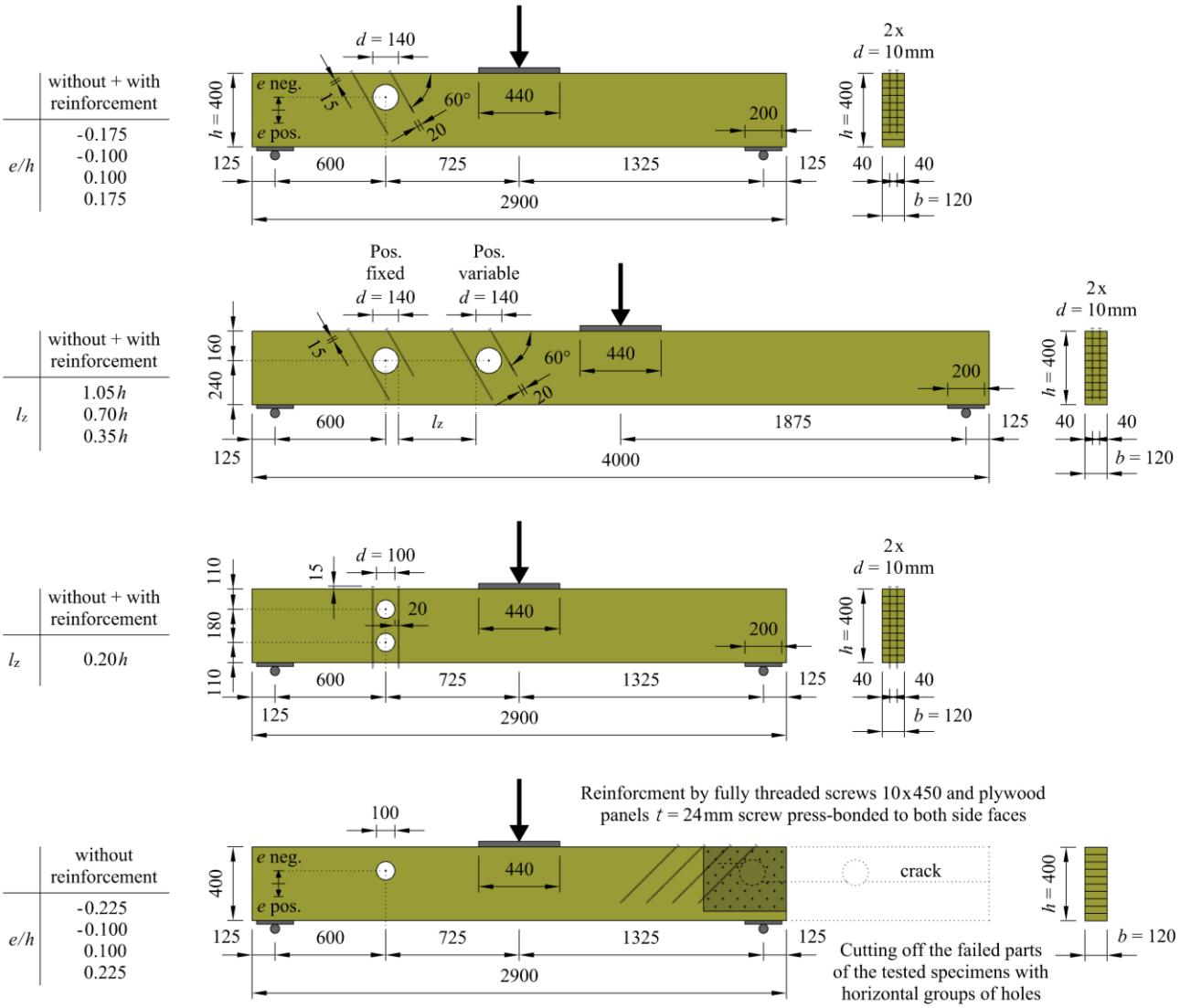

Figure 2: *Test configurations for investigation of the parameters eccentricity, clear distance and effect of reinforcement*

2.2 RESULTS

2.2.1 Failure characteristics

In most cases the following failure characteristics, following three steps of failure, could be observed, see Figure 3.

The first sign of a beginning failure was an initial cracking in the middle of the cross-sectional width due to tension perpendicular to the grain (crack initiation). After that the increasing load led to a crack growth across the cross-sectional width to both side faces (full crack). The last step could be characterized by a progressive failure in the longitudinal direction up to the beam end due to tension perpendicular to the grain and/or shear (ultimate load).

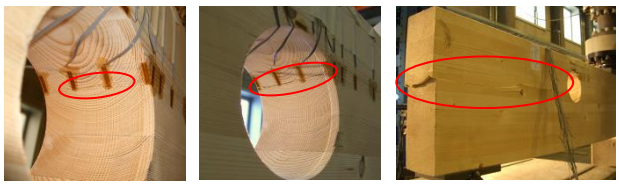

Figure 3: *Stepwise failure characteristics (left: crack initiation; middle: full crack; right: ultimate load)*

Due to this fact, the test results given in the following were differentiated according to the aforementioned steps of failure. Specific failure characteristics of the individual configurations are only discussed, if they differed from the characteristics presented in this section.

2.2.2 Test results

The test results are presented separately for each configuration. To understand the underlying values in detail a summary of the results is listed in Table 1.

- Single holes arranged eccentrically ($d/h = 0.35$)

In the unreinforced state only a marginal influence of the eccentricity could be observed for all three levels of failure, see Figure 4. From the crack initiation to ultimate load, a load increase of around 20% can be seen. The *CoV* for the first step of failure (crack initiation) is higher than for the following steps of failure. This finding is valid for all tested configurations and mirrors the findings reported in [3].

In the reinforced state - compared to the unreinforced state - load increases of around 40% were achieved at the level of crack initiation. At the levels of full crack and ultimate load up to 100% load increase was observed, dependent on the eccentricity. Clearly visible are the decreasing loads for the levels of full crack and ultimate load, when grouping the eccentricity of the holes from the edge under compressive bending stresses to the edge under tension bending stresses. At the eccentricity $e/h = +0.175$, an additional failure mode in the form of a bending tension failure between the lower edge of the hole and the lower edge of the beam, in the area penetrated by the fully threaded screws, occurred.

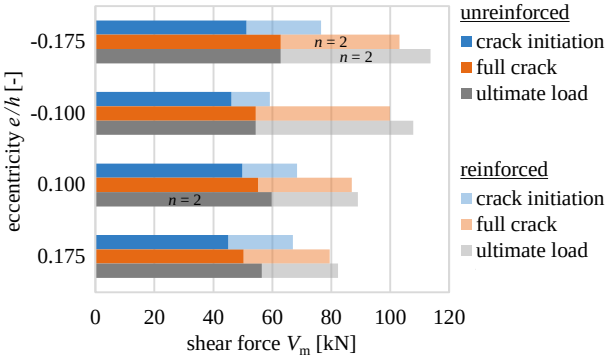

Figure 4: *Test data (mean values) of holes arranged eccentrically (d/h = 0.35)*

- Single holes arranged eccentrically ($d/h = 0.25$)

For the configurations with the smaller hole diameter in the unreinforced state a more pronounced influence of the eccentricity was determined, with higher loads for larger eccentricities, see Figure 5. However, due to the partially unexpected low load values, only the results of the two new specimens are used for further considerations, see also section 3.4. Presumably the first testing process caused a kind of pre-damage, which resulted in lower load values in the repeated testing process.

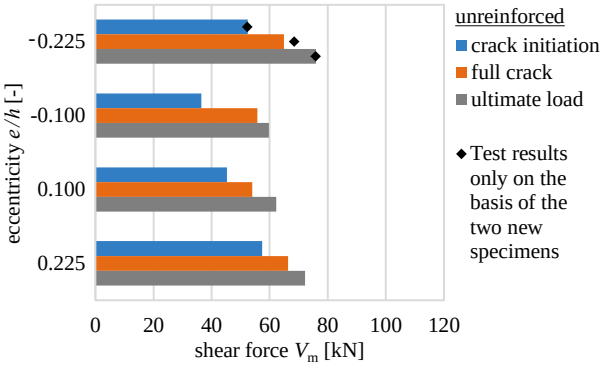

Figure 5: *Test data (mean values) of holes arranged eccentrically (d/h = 0.25)*

- Groups of holes arranged in horizontal direction ($d/h = 0.35$)

In the unreinforced state a decreasing clear distance between the holes resulted in decreasing loads and thereby in an increasing mutual influence of the two holes for all three levels of failure, see Figure 6. Compared to the configuration of an individual hole with the same eccentricity, the group arrangement with the largest clear distance "$l_z = 1.05h$" failed at only negligibly lower loads.

The percentage load increases in the reinforced state at the level of crack initiation are in a similar range compared to those of the reinforced individual holes. At the levels full crack and ultimate load they are, however, in most cases limited due to the premature failure of the beams in global bending/shear.

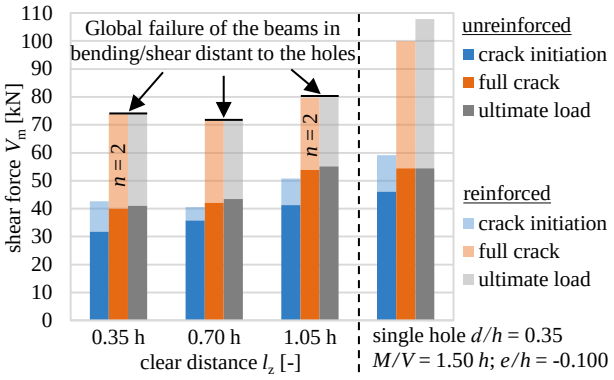

Figure 6: *Test data (mean values) of groups of holes arranged in horizontal direction (d/h = 0.35)*

- Groups of holes arranged in vertical direction (d/h = 0.25)

Compared to single unreinforced holes with the same eccentricity, the failure of the vertical groups appeared at negligibly lower loads, i.e. the mutual influence in this configuration was small, see Figure 7.

In the reinforced state diverse failure modes could be observed: shear failure in the region of the holes up to the beam end/bending tension failure at the lower edge of the cross-section in the area of the screws/combined tension perpendicular to the grain - bending tension - shear failure. The percentage load increases are small in comparison to the individual holes reinforced with inclined fully threaded screws.

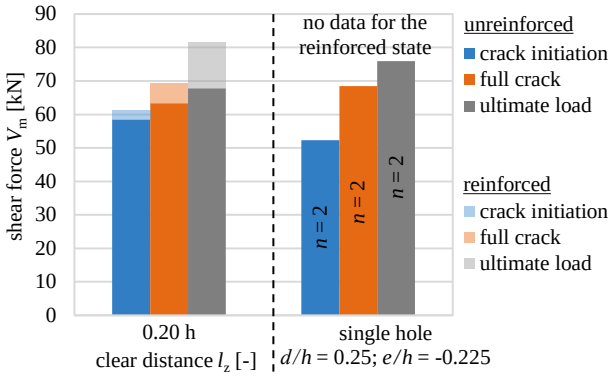

Figure 7: *Test data (mean values) of the groups of holes arranged in vertical direction (d/h = 0.25)*

Table 1: *Test results (c.i.: crack initiation; f.c.: full crack; u.l.: ultimate load)*

Single holes arranged eccentrically (d/h = 0.35)

without reinforcement

	e/h = -0.175			e/h = -0.100			e/h = 0.100			e/h = 0.175		
	c. i.	f. c.	u. l.	c. i.	f. c.	u. l.	c. i.	f. c.	u. l.	c. i.	f. c.	u. l.
no. 1	38.0	58.9	58.9	40.2	56.9	56.9	48.4	51.1	-	56.1	56.1	56.1
no. 2	62.3	72.6	72.6	42.5	50.8	50.8	53.2	60.9	60.9	33.8	44.9	63.6
no. 3	53.4	57.2	57.2	55.7	55.7	55.7	48.0	53.3	58.8	45.4	49.9	49.9
V_m [kN]	51.2	62.9	62.9	46.1	54.4	54.4	49.9	55.1	59.8	45.1	50.3	56.5
CoV [%]	24.0	13.4	13.4	18.1	5.9	5.9	5.8	9.3	2.4	24.6	11.1	12.1

with reinforcement

	e/h = -0.175			e/h = -0.100			e/h = 0.100			e/h = 0.175		
	c. i.	f. c.	u. l.	c. i.	f. c.	u. l.	c. i.	f. c.	u. l.	c. i.	f. c.	u. l.
no. 1	78.5	102.2	115.0	51.2	104.3	109.7	83.0	91.6	91.6	65.0	77.0	78.0
no. 2	85.3	-	-	56.9	103.8	103.8	73.2	89.8	89.8	67.9	79.7	83.4
no. 3	66.0	104.1	112.4	69.3	91.7	110.1	49.1	79.5	85.6	67.9	81.8	85.6
V_m [kN]	76.6	103.1	113.7	59.1	99.9	107.8	68.5	87.0	89.0	66.9	79.5	82.3
CoV [%]	12.8	1.3	1.6	15.6	7.1	3.2	25.5	7.5	3.5	2.5	3.0	4.7

Groups of holes arranged in horizontal direction (d/h = 0.35)

without reinforcement

	l_z = 0.35 h			l_z = 0.70 h			l_z = 1.05 h		
	c. i.	f. c.	u. l.	c. i.	f. c.	u. l.	c. i.	f. c.	u. l.
no. 1	31.1	37.3	39.2	36.2	42.6	45.7	48.0	49.7	49.7
no. 2	42.5	42.9	44.0	36.2	41.4	42.2	49.2	56.9	60.0
no. 3	21.8	39.8	39.8	35.0	42.3	42.3	26.5	55.1	55.8
V_m [kN]	31.8	40.0	41.0	35.8	42.1	43.4	41.2	53.9	55.2
CoV [%]	32.6	7.0	6.4	2.0	1.6	4.6	31.0	6.9	9.4

with reinforcement

	l_z = 0.35 h			l_z = 0.70 h			l_z = 1.05 h		
	c. i.	f. c.	u. l.	c. i.	f. c.	u. l.	c. i.	f. c.	u. l.
no. 1	34.3	-	66.9	40.5	-	65.3	42.5	76.5	89.2
no. 2	40.1	52.8	83.3	45.8	-	84.1	56.2	-	75.4
no. 3	53.6	-	71.8	35.6	-	65.3	53.6	-	74.4
V_m [kN]	42.6	-	74.0	40.6	-	71.6	50.7	-	79.7
CoV [%]	23.2	-	11.3	12.6	-	15.1	14.3	-	10.3

global failure in bending/shear distant to the holes

Groups of holes arranged in vertical direction (d/h = 0.25)

without reinforcement

	l_z = 0.20 h		
	c. i.	f. c.	u. l.
no. 1	71.0	71.0	71.0
no. 2	60.8	66.5	66.5
no. 3	43.7	52.4	65.9
V_m [kN]	58.5	63.3	67.8
CoV [%]	23.6	15.3	4.1

with reinforcement

	l_z = 0.20 h		
	c. i.	f. c.	u. l.
no. 1	60.6	76.3	76.3
no. 2	60.9	69.2	84.3
no. 3	62.5	62.5	84.2
V_m [kN]	61.3	69.3	81.6
CoV [%]	1.7	9.9	5.6

Single holes arranged eccentrically (d/h = 0.25)

without reinforcement

	e/h = -0.225			e/h = -0.100			e/h = 0.100			e/h = 0.225		
	c. i.	f. c.	u. l.	c. i.	f. c.	u. l.	c. i.	f. c.	u. l.	c. i.	f. c.	u. l.
no. 1	59.6	71.0	79.3	36.0	51.6	55.7	43.5	48.7	55.7	52.6	59.9	73.4
no. 2	52.7	57.9	76.0	36.7	55.2	58.5	50.2	60.4	67.0	70.0	70.0	71.8
no. 3	45.0	66.0	72.5	36.7	60.6	65.1	42.3	52.8	64.1	49.8	69.2	71.4
V_m [kN]	52.4	65.0	75.9	36.5	55.8	59.8	45.3	54.0	62.3	57.5	66.4	72.2
CoV [%]	13.9	10.1	4.5	1.1	8.1	8.0	9.4	11.0	9.4	19.1	8.4	1.5

new specimen which were tested for the first time

3 NUMERICAL INVESTIGATIONS

3.1 NUMERICAL MODEL

Numerical investigations were realized in order to estimate the load-bearing capacities of the tested glulam beams as well as to investigate the general behaviour of round holes in glulam beams with/without the effect of reinforcement by fully threaded screws. A two dimensional simulation model with orthotropic material properties of glulam according DIN EN 14080:2013-09 (mean values) was set up in the FEM-software ANSYS 14.5, see Figure 8. Beam elements featuring the isotropic material behaviour of steel and a circular cross section, corresponding to the core diameter of the screws, were used for simulating the reinforcing elements. The interaction between the screws and the timber was modelled by spring elements in axial (withdrawal stiffness k_{ax}) and lateral direction (embedding stiffness k_{ser}) of the screw axis. Embedment lengths were determined by considering the locations of the maximum tension stresses perpendicular to the grain at the hole edge in the unreinforced state. The whole computation was performed on the basis of linear elastic behaviour.

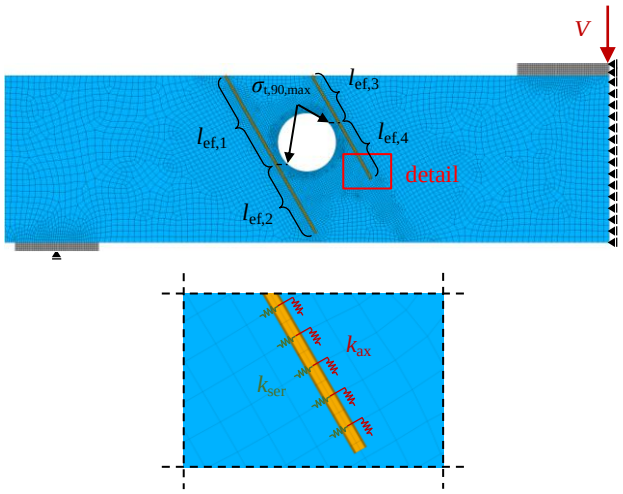

Figure 8: *Numerical model (top: entire model; bottom: detail of the interaction between screw and timber)*

3.2 STIFFNESS OF REINFORCEMENT IN AXIAL AND LATERAL DIRECTION

For the embedding stiffness, k_{ser}, values for different angles between screw axis and fibre direction could be derived from [4]. Due to the significant influence of the magnitude of the withdrawal stiffness, k_{ax}, on the load-bearing capacities, it was decided to realize separate tests.

Referring to the approach reported in [5], the following parameters were investigated:

- d = 10 mm
- l_{ef} = 80 mm / 120 mm / 180 mm
- α = 45° / 60° / 90°

In total the test program encompassed 45 specimens, 5 specimens per configuration. The material used was GL 28h. The average density of the specimens was $\rho_m = 471\,kg/m^3$ (CoV = 4.7%).

Assuming that the stiffness in axial direction features the same behaviour in tension and compression, in a first step a compressive load was applied only to the wooden cross-section of the specimens according the test set up in Figure 9. Thereby the length variations of the screws between the end parts, penetrating through the holes in the steel plates, were measured, see Figure 9.

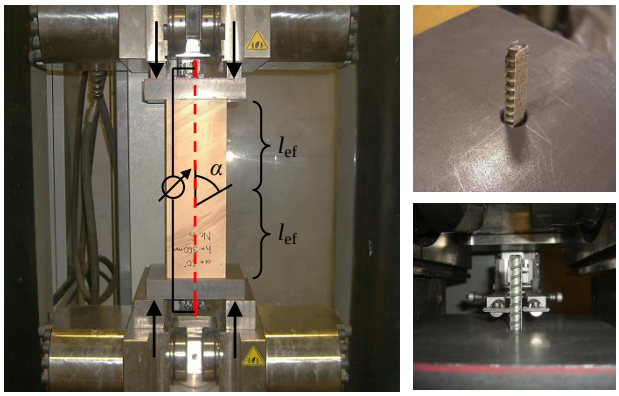

Figure 9: *Test set up for investigation of the withdrawal stiffness k_{ax}*

Results of these tests are shown in Figure 10 for the example of an angle between screw axis and fibre direction of $\alpha = 60°$. Each curve within the load range $F = 10\,kN$ to $F = 25\,kN$ was approximated by a linear function. Afterwards the mean values of the gradients (force per length variation of the screw) out of the five single tests were determined.

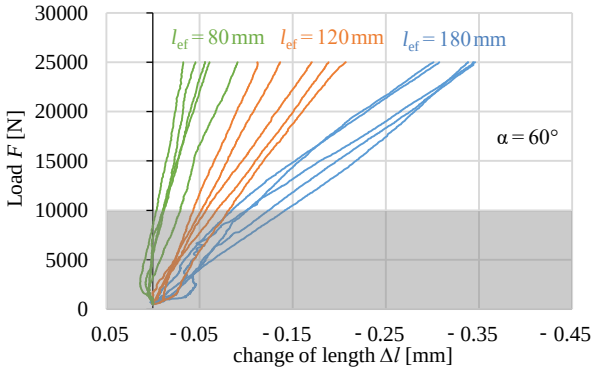

Figure 10: *Results of the tests for the example of an angle between screw axis and fibre direction of $\alpha = 60°$*

In a second step simulations were done by using the numerical model shown in Figure 11. Assuming a constant distribution of the withdrawal stiffness along the embedment length l_{ef}, the stiffness values of the springs were adjusted iteratively, so that the length variations of the screws in the tests and in the simulations matched.

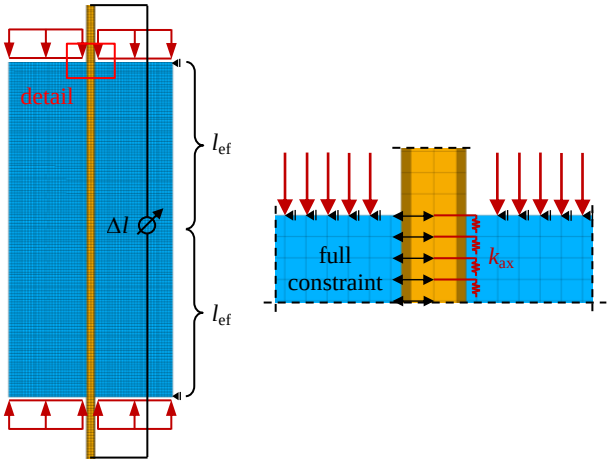

Figure 11: *Numerical model for the determination of values of the withdrawal stiffness k_{ax}*

Results of the simulations and approximated equations for the mean withdrawal stiffness k_{ax} are shown in Figure 12. The approximated equations correspond to the equation derived in [4], adjusted in the numerical prefactor.

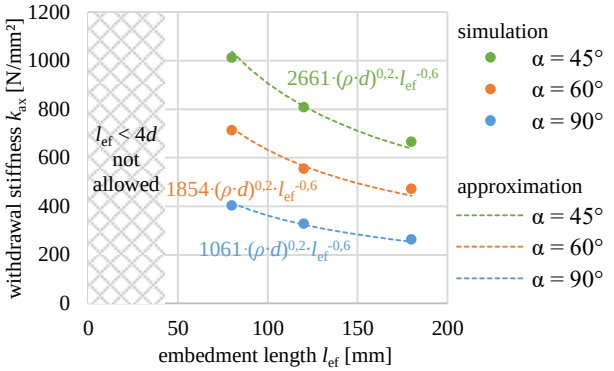

Figure 12: *Determined values of the withdrawal stiffness k_{ax}*

3.3 ESTIMATION OF LOAD-BEARING CAPACITIES

For estimating load-bearing capacities on the basis of the aforementioned numerical model and stiffness characteristics the Weibull based design approach reported in [3], applying equations (1) to (3), was used.

$$\sigma_{t,90,max} = k_{dis}\, k_{vol}\, f_{t,90,m} \tag{1}$$

$$k_{dis} = \left(\frac{V}{V^*}\right)^{\frac{1}{k}} \quad where\ V^* = \int \left(\frac{\sigma_{t,90}(x,y,z)}{\sigma_{t,90,max}}\right)^k dV \tag{2}$$

$$k_{vol} = \left(\frac{V_0}{V}\right)^{\frac{1}{k}} \quad where\ V_0 = 0{,}01 m^3\ and\ k = 5 \tag{3}$$

The required values for equations (1) to (3), the maximum stress perpendicular to the grain $\sigma_{t,90,max}$ and the stressed volumes V in tension perpendicular to the grain, are illustrated in Figure 13.

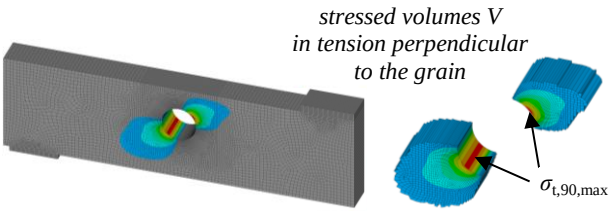

Figure 13: *Maximum stresses $\sigma_{t,90,max}$ and stressed volumes V in tension perpendicular to the grain*

The determination of the load-bearing capacities was performed at the level of mean values using a strength value perpendicular to the grain $f_{t,90,m}$ = 0,83 N/mm² (mean value of test results reported in [6] and [7]). As a result a failure perpendicular to the grain can be estimated with this approach. This corresponds to the second step of the failure characteristics, the crack growth reaching both side faces (full crack).

3.4 COMPARISON BETWEEN TESTS AND SIMULATION

For verification of the numerical model and the determined values of the withdrawal stiffness k_{ax}, strain measurements were carried out in some reinforcing elements. Figure 14 shows the principal application of a strain gauge.

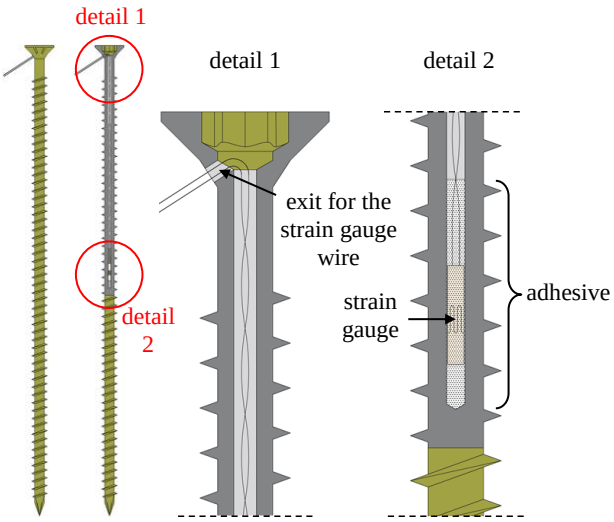

Figure 14: *Strain gauge application in the screws*

Starting from the head of the screw, a centric drill hole of a diameter 2 mm was produced. After inserting an appropriate epoxy resin adhesive, a cylindrical strain gauge was placed in the fluid adhesive. The wires of the strain gauges were led out through a lateral drilling below the head, so that the application of the strain gauge could be realized before setting the screw.
A comparison between the axial forces in the screws derived by strain measurement in the tests and the simulation is illustrated in Figure 15. Due of the fact, that the numerical simulations were done only in the linear elastic range, a comparison is possible only up to the load level of beginning failure (crack initiation).

Nevertheless, good agreement in this range confirms the validity of the chosen methods.

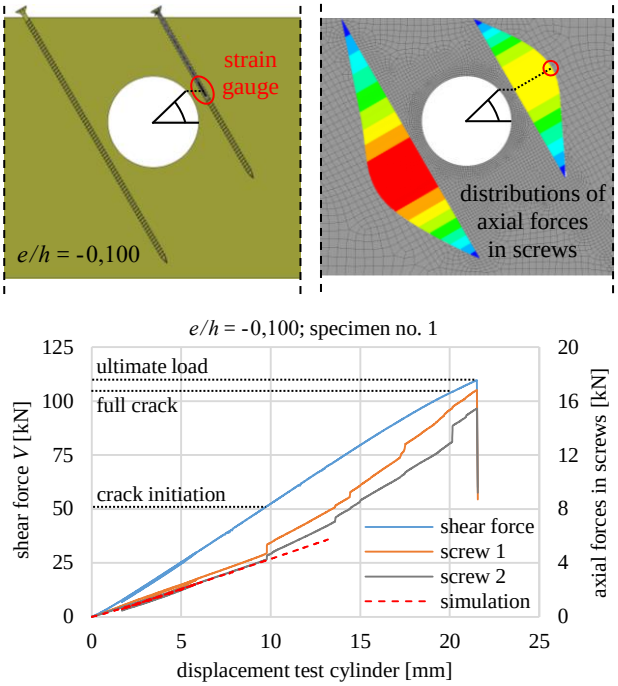

Figure 15: *Strain measurement in screws (top left: situation; top right: simulation; bottom: comparison of test results and simulation)*

- Single holes arranged eccentrically ($d/h = 0.35$)

In Figure 16 a comparison between the test data (mean values) and the estimated load-bearing capacities is illustrated. In the unreinforced state good agreement can be stated continuously, in the reinforced state the estimated load-bearing capacities are slightly too low.

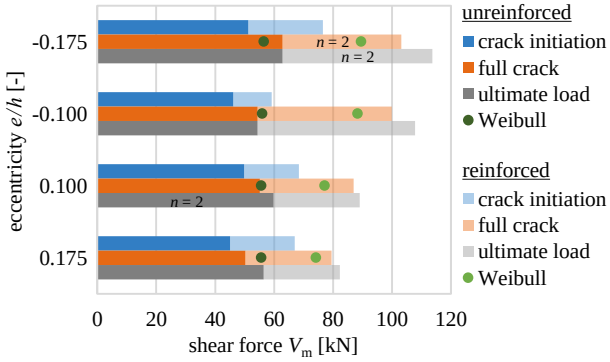

Figure 16: *Comparison of test data (mean values) and estimated load-bearing capacities of holes arranged eccentrically (d/h = 0.35)*

The reason for the decreasing test results, when grouping the eccentricity of the holes from the edge under compressive bending stresses to the edge under tension bending stresses, can be derived from Figure 17. In dependence of the eccentricity the locations of the maximum tension stresses perpendicular to the grain at the hole edge – and in general the distributions of these stresses in the periphery – differ. As a result, the distances between these locations and the reinforcing elements, which were applied at a constant angle $\alpha = 60°$, differ. The larger this distance the slighter the reinforcing effect. The influence of this parameter is discussed in detail in the following section.

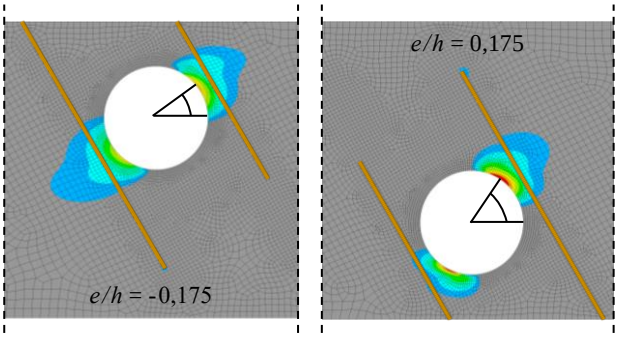

Figure 17: *Distributions of stresses in tension perpendicular to the grain for two different configurations in the reinforced state at the same load level*

- Single holes arranged eccentrically ($d/h = 0.25$)

The partially unexpected low values mentioned in section 2.2.2 are illustrated for these configurations in Figure 18. A comparison of all test data and the estimated load-bearing capacities shows a continuous discrepancy. However, the test results of the two new specimens and the estimated values show good agreement.

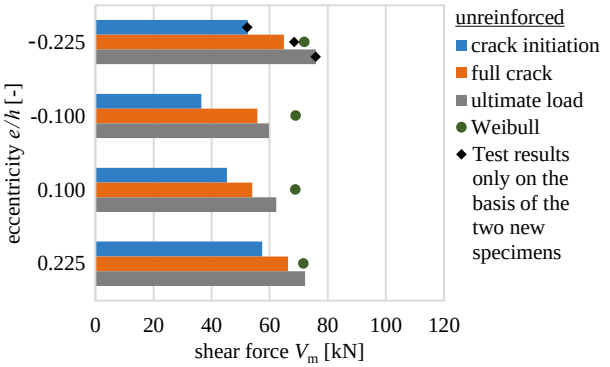

Figure 18: *Comparison of test data (mean values) and estimated load-bearing capacities of holes arranged eccentrically (d/h = 0.25)*

- Groups of holes arranged in horizontal direction ($d/h = 0.35$)

While in the unreinforced state test results and estimated values are also in good agreement, in the reinforced state no clear statement is possible because of the different failure modes, see Figure 19. However, the estimated load-bearing capacities tend to be also slightly too low.

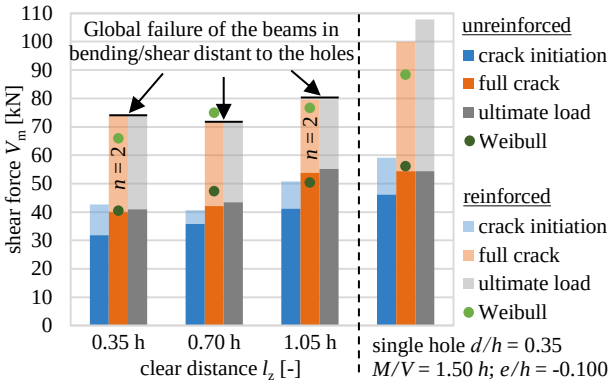

Figure 19: *Comparison of test data (mean values) and estimated load-bearing capacities of groups of holes arranged in horizontal direction ($d/h = 0.35$)*

- Groups of holes arranged in vertical direction ($d/h = 0.25$)

The comparison in the case of the vertical group shows good agreement in the unreinforced as well as in the reinforced state, see Figure 20.

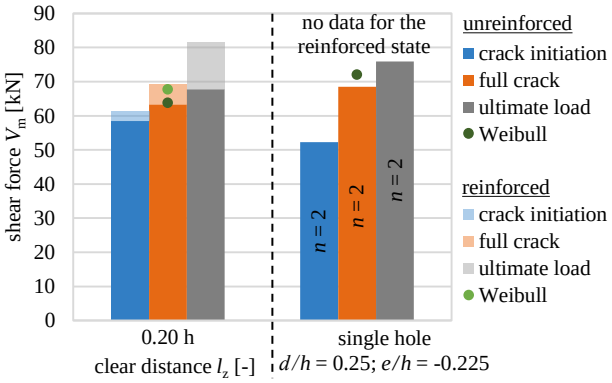

Figure 20: *Comparison of test data (mean values) and estimated load-bearing capacities of groups of holes arranged in vertical direction ($d/h = 0.25$)*

The comparatively low effect of the reinforcing elements can be explained by the distribution of the tension stresses perpendicular to the grain illustrated in Figure 21.

In the unreinforced state the upper hole was decisive for the test results. Due to the comparatively small distance between the location of the maximum tension stresses perpendicular to the grain and the screws, the reinforcing effect is obvious for this hole.

In contrast, a comparison of the tension stresses at the lower hole in the unreinforced and reinforced state shows only a slight reinforcing effect. Because of the larger distance between the location of the maximum stresses and the screws, that hole was decisive in the reinforced state, resulting in a comparatively slight load increase of the reinforced vertical group.

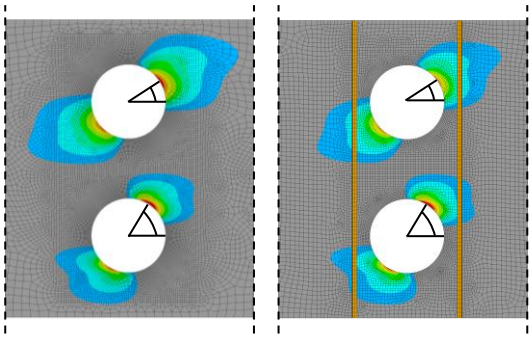

Figure 21: *Distributions of tension stresses perpendicular to the grain at the same load level (left: unreinforced state; right: reinforced state)*

3.5 PARAMETRIC STUDIES

In parametric studies based on the configuration "single holes arranged eccentrically ($d/h = 0.35$)" the influence of the parameters *angle* α between screw axis and fibre direction as well as *distance* a between screw axis and hole edge was quantified.

- Angle α between screw axis and fibre direction

In Figure 22 the estimated load-bearing capacities are illustrated in the unreinforced state as well as in the reinforced state for the three different inclinations of the screws investigated in section 3.2. Thereby, the distance a between screw axis and hole edge was kept constant at 20 mm. While for locations of the holes in the area under compression bending stresses the chosen inclination in the tests $\alpha = 60°$ reveals the highest values, for locations of the holes in the bending tension part an inclination of $\alpha = 45°$ would have been the better choice. Clearly visible are the higher load-bearing capacities in the cases of inclined application of the reinforcing elements in contrast to an inclination of $\alpha = 90°$.

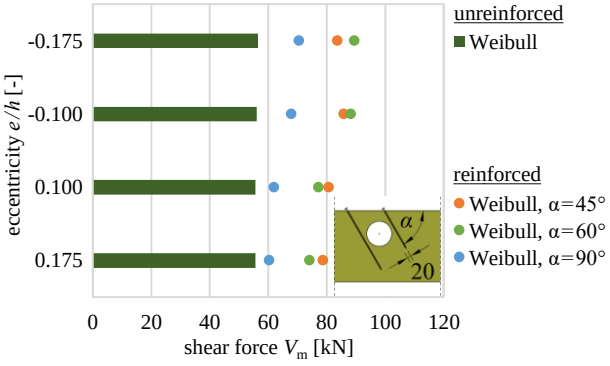

Figure 22: *Load-bearing capacities in dependency of the angle α between screw axis and fibre direction*

- Distance a between screw axis and hole edge

Figure 23 shows the significant influence of this parameter for the chosen eccentricities. An increasing distance a results in decreasing load-bearing capacities, whereby the changes between the single steps decrease with an increasing distance. For very large distances the behaviour converges against the values obtained in the unreinforced state. The angle between screw axis and fibre direction was throughout $\alpha = 60°$. The trend for other inclinations will be comparable, however, the

values will differ because of the differing distances between reinforcing element and maximum stress in tension perpendicular to the grain.

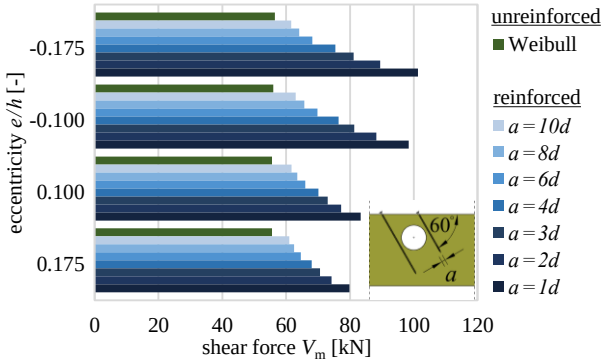

Figure 23: *Load-bearing capacities in dependency of the distance a between screw axis and hole edge*

4 CONCLUSIONS AND OUTLOOK

The results of the experimental investigations show good agreement with the numerical investigations and corresponding Weibull based design approach. Strain gauge measurements in reinforcing elements confirm the validity of the chosen methods.

The positive influence of fully threaded screws applied as reinforcement at an angle to the grain and as close as possible to the location of maximum tensile stresses perpendicular to the grain was shown.

The results of the numerical investigations are influenced by the axial withdrawal stiffness of the fully threaded screws. Hence, this parameter was experimentally derived for common cases of application.

Further numerical investigations in combination with full scale tests will be realized to provide a larger basis for deriving a general statement on the influence of eccentricity of holes as well as distance between holes.

REFERENCES

[1] Kolb H., Epple A.: Verstärkung von durchbrochenen Brettschichtbindern, Schlussbericht Forschungsvorhaben I.4-34810, Forschungs- und Materialprüfungsanstalt Baden-Württemberg, Stuttgart, 1985

[2] ETA-12/0114: SPAX self-tapping screws, ETA-Danmark A/S, 2012

[3] Höfflin L.: Runde Durchbrüche in Brettschichtholzträgern – Experimentelle und theoretische Untersuchungen, PhD thesis, MPA Universität Stuttgart, Schriftenreihe Heft 90, Stuttgart, 2005

[4] Blaß H. J., Bejtka I., Uibel T.: Tragfähigkeit von Verbindungen mit selbstbohrenden Holzschrauben mit Vollgewinde, Band 4 der Reihe Karlsruher Berichte zum Ingenieurholzbau, KIT Scientific Publishing, Karlsruhe, 2006

[5] Mestek P., Winter S.: Konzentrierte Lasteinleitung in Brettsperrholzkonstruktionen - Verstärkungsmaßnahmen, AiF Forschungsvorhaben Nr. 15892 – Schlussbericht, Lehrstuhl für Holzbau und Baukonstruktion, TU München, 2011

[6] Aicher S., Dill-Langer G.: DOL effect in tension perpendicular to the grain of glulam depending on service classes and volume, CIB-W18 Meeting 30, Paper No. CIB-W18/30-9-1, Vancouver, 1997

[7] Blaß H. J., Ehlbeck J., Schmid M.: Ermittlung der Querzugfestigkeit von Voll- und Brettschichtholz, Versuchsanstalt für Stahl, Holz und Steine, Abteilung Ingenieurholzbau, Universität Karlsruhe, 1998